

**Azimuthal anisotropy of K_S^0 and $\Lambda + \bar{\Lambda}$ production at mid-rapidity from Au+Au collisions at
 $\sqrt{s_{\text{NN}}} = 130 \text{ GeV}$**

C. Adler¹¹, Z. Ahammed²³, C. Allgower¹², J. Amonett¹⁴, B.D. Anderson¹⁴, M. Anderson⁵, G.S. Averichev⁹, J. Balewski¹², O. Barannikova^{9,23}, L.S. Barnby¹⁴, J. Baudot¹³, S. Bekele²⁰, V.V. Belaga⁹, R. Bellwied³¹, J. Berger¹¹, H. Bichsel³⁰, A. Billmeier³¹, L.C. Bland², C.O. Blyth³, B.E. Bonner²⁴, A. Boucham²⁶, A. Brandin¹⁸, A. Bravar², R.V. Cadman¹, H. Caines²⁰, M. Calderón de la Barca Sánchez², A. Cardenas²³, J. Carroll¹⁵, J. Castillo²⁶, M. Castro³¹, D. Cebra⁵, P. Chaloupka²⁰, S. Chattopadhyay³¹, Y. Chen⁶, S.P. Chernenko⁹, M. Cherney⁸, A. Chikanian³³, B. Choi²⁸, W. Christie², J.P. Coffin¹³, T.M. Cormier³¹, J.G. Cramer³⁰, H.J. Crawford⁴, W.S. Deng², A.A. Derevschikov²², L. Didenko², T. Dietel¹¹, J.E. Draper⁵, V.B. Dunin⁹, J.C. Dunlop³³, V. Eckardt¹⁶, L.G. Efimov⁹, V. Emelianov¹⁸, J. Engelage⁴, G. Eppley²⁴, B. Erazmus²⁶, P. Fachini², V. Faine², K. Filimonov¹⁵, E. Finch³³, Y. Fisyak², D. Flierl¹¹, K.J. Foley², J. Fu^{15,32}, C.A. Gagliardi²⁷, N. Gagunashvili⁹, J. Gans³³, L. Gaudichet²⁶, M. Germain¹³, F. Geurts²⁴, V. Ghazikhanian⁶, O. Grachov³¹, V. Grigoriev¹⁸, M. Guedon¹³, E. Gushin¹⁸, T.J. Hallman², D. Hardtke¹⁵, J.W. Harris³³, T.W. Henry²⁷, S. Heppelmann²¹, T. Herston²³, B. Hippolyte¹³, A. Hirsch²³, E. Hjort¹⁵, G.W. Hoffmann²⁸, M. Horsley³³, H.Z. Huang⁶, T.J. Humanic²⁰, G. Igo⁶, A. Ishihara²⁸, Yu.I. Ivanshin¹⁰, P. Jacobs¹⁵, W.W. Jacobs¹², M. Janik²⁹, I. Johnson¹⁵, P.G. Jones³, E.G. Judd⁴, M. Kaneta¹⁵, M. Kaplan⁷, D. Keane¹⁴, J. Kiryluk⁶, A. Kisiel²⁹, J. Klay¹⁵, S.R. Klein¹⁵, A. Klyachko¹², A.S. Konstantinov²², M. Kopytine¹⁴, L. Kotchenda¹⁸, A.D. Kovalenko⁹, M. Kramer¹⁹, P. Kravtsov¹⁸, K. Krueger¹, C. Kuhn¹³, A.I. Kulikov⁹, G.J. Kunde³³, C.L. Kunz⁷, R.Kh. Kutuev¹⁰, A.A. Kuznetsov⁹, L. Lakehal-Ayat²⁶, M.A.C. Lamont³, J.M. Landgraf², S. Lange¹¹, C.P. Lansdell²⁸, B. Lasiuk³³, F. Laue², A. Lebedev², R. Lednický⁹, V.M. Leontiev²², M.J. LeVine², Q. Li³¹, S.J. Lindenbaum¹⁹, M.A. Lisa²⁰, F. Liu³², L. Liu³², Z. Liu³², Q.J. Liu³⁰, T. Ljubicic², W.J. Llope²⁴, G. LoCurto¹⁶, H. Long⁶, R.S. Longacre², M. Lopez-Noriega²⁰, W.A. Love², T. Ludlam², D. Lynn², J. Ma⁶, R. Majka³³, S. Margetis¹⁴, C. Markert³³, L. Martin²⁶, J. Marx¹⁵, H.S. Matis¹⁵, Yu.A. Matulenko²², T.S. McShane⁸, F. Meissner¹⁵, Yu. Melnick²², A. Meschanin²², M. Messer², M.L. Miller³³, Z. Milosevich⁷, N.G. Minaev²², J. Mitchell²⁴, V.A. Moiseenko¹⁰, C.F. Moore²⁸, V. Morozov¹⁵, M.M. de Moura³¹, M.G. Munhoz²⁵, J.M. Nelson³, P. Nevski², V.A. Nikitin¹⁰, L.V. Nogach²², B. Norman¹⁴, S.B. Nurushev²², G. Odyniec¹⁵, A. Ogawa²¹, V. Okorokov¹⁸, M. Oldenburg¹⁶, D. Olson¹⁵, G. Paic²⁰, S.U. Pandey³¹, Y. Panebratsev⁹, S.Y. Panitkin², A.I. Pavlinov³¹, T. Pawlak²⁹, V. Perevoztchikov², W. Peryt²⁹, V.A. Petrov¹⁰, M. Planinic¹², J. Pluta²⁹, N. Porile²³, J. Porter², A.M. Poskanzer¹⁵, E. Potrebenikova⁹, D. Prindle³⁰, C. Pruneau³¹, J. Putschke¹⁶, G. Rai¹⁵, G. Rakness¹², O. Ravel²⁶, R.L. Ray²⁸, S.V. Razin^{9,12}, D. Reichhold⁸, J.G. Reid³⁰, F. Retiere¹⁵, A. Ridiger¹⁸, H.G. Ritter¹⁵, J.B. Roberts²⁴, O.V. Rogachevski⁹, J.L. Romero⁵, A. Rose³¹, C. Roy²⁶, V. Rykov³¹, I. Sakrejda¹⁵, S. Salur³³, J. Sandweiss³³, A.C. Saulys², I. Savin¹⁰, J. Schambach²⁸, R.P. Scharenberg²³, N. Schmitz¹⁶, L.S. Schroeder¹⁵, A. Schüttauf¹⁶, K. Schweda¹⁵, J. Seger⁸, D. Seliverstov¹⁸, P. Seyboth¹⁶, E. Shahaliev⁹, K.E. Shestermanov²², S.S. Shimanskii⁹, V.S. Shvetcov¹⁰, G. Skoro⁹, N. Smirnov³³, R. Snellings¹⁵, P. Sorensen⁶, J. Sowinski¹², H.M. Spinka¹, B. Srivastava²³, E.J. Stephenson¹², R. Stock¹¹, A. Stolpovsky³¹, M. Strikhanov¹⁸, B. Stringfellow²³, C. Struck¹¹, A.A.P. Suade³¹, E. Sugarbaker²⁰, C. Suire², M. Šumbera²⁰, B. Surrow², T.J.M. Symons¹⁵, A. Szanto de Toledo²⁵, P. Szarwas²⁹, A. Tai⁶, J. Takahashi²⁵, A.H. Tang¹⁴, J.H. Thomas¹⁵, M. Thompson³, V. Tikhomirov¹⁸, M. Tokarev⁹, M.B. Tonjes¹⁷, T.A. Trainor³⁰, S. Trentalange⁶, R.E. Tribble²⁷, V. Trofimov¹⁸, O. Tsai⁶, T. Ullrich², D.G. Underwood¹, G. Van Buren², A.M. VanderMolen¹⁷, I.M. Vasilevski¹⁰, A.N. Vasiliev²², S.E. Vigdor¹², S.A. Voloshin³¹, F. Wang²³, H. Ward²⁸, J.W. Watson¹⁴, R. Wells²⁰, G.D. Westfall¹⁷, C. Whitten Jr.⁶, H. Wieman¹⁵, R. Willson²⁰, S.W. Wissink¹², R. Witt³², J. Wood⁶, N. Xu¹⁵, Z. Xu², A.E. Yakutin²², E. Yamamoto¹⁵, J. Yang⁶, P. Yepes²⁴, V.I. Yurevich⁹, Y.V. Zanevski⁹, I. Zborovský⁹, H. Zhang³³, W.M. Zhang¹⁴, R. Zoukarneev¹⁰, A.N. Zubarev⁹

(STAR Collaboration)

¹*Argonne National Laboratory, Argonne, Illinois 60439*

²*Brookhaven National Laboratory, Upton, New York 11773*

³*University of Birmingham, Birmingham, United Kingdom*

⁴*University of California, Berkeley, California 94720*

⁵*University of California, Davis, California 95616*

⁶*University of California, Los Angeles, California 90095*

⁷*Carnegie Mellon University, Pittsburgh, Pennsylvania 15213*

⁸*Creighton University, Omaha, Nebraska 68178*

⁹*Laboratory for High Energy (JINR), Dubna, Russia*

¹⁰*Particle Physics Laboratory (JINR), Dubna, Russia*

¹¹*University of Frankfurt, Frankfurt, Germany*

- ¹²*Indiana University, Bloomington, Indiana 47408*
¹³*Institut de Recherches Subatomiques, Strasbourg, France*
¹⁴*Kent State University, Kent, Ohio 44242*
¹⁵*Lawrence Berkeley National Laboratory, Berkeley, California 94720*
¹⁶*Max-Planck-Institut fuer Physik, Munich, Germany*
¹⁷*Michigan State University, East Lansing, Michigan 48824*
¹⁸*Moscow Engineering Physics Institute, Moscow Russia*
¹⁹*City College of New York, New York City, New York 10031*
²⁰*Ohio State University, Columbus, Ohio 43210*
²¹*Pennsylvania State University, University Park, Pennsylvania 16802*
²²*Institute of High Energy Physics, Protvino, Russia*
²³*Purdue University, West Lafayette, Indiana 47907*
²⁴*Rice University, Houston, Texas 77251*
²⁵*Universidade de Sao Paulo, Sao Paulo, Brazil*
²⁶*SUBATECH, Nantes, France*
²⁷*Texas A & M, College Station, Texas 77843*
²⁸*University of Texas, Austin, Texas 78712*
²⁹*Warsaw University of Technology, Warsaw, Poland*
³⁰*University of Washington, Seattle, Washington 98195*
³¹*Wayne State University, Detroit, Michigan 48201*
³²*Institute of Particle Physics, Wuhan, Hubei 430079 China and*
³³*Yale University, New Haven, Connecticut 06520*

(Dated: April 29, 2002)

We report STAR results on the azimuthal anisotropy parameter v_2 for strange particles K_S^0 , Λ and $\bar{\Lambda}$ at mid-rapidity in Au+Au collisions at $\sqrt{s_{NN}} = 130$ GeV at RHIC. The value of v_2 as a function of transverse momentum of the produced particles p_t and collision centrality is presented for both particles up to $p_t \sim 3.0$ GeV/c. A strong p_t dependence in v_2 is observed up to 2.0 GeV/c. The v_2 measurement is compared with hydrodynamic model calculations. The physics implications of the p_t integrated v_2 magnitude as a function of particle mass are also discussed.

PACS numbers: 25.75.Wd, 25.75.Ld

Measurements of azimuthal anisotropies in the transverse momentum distribution of particles can probe early stages of ultra-relativistic heavy-ion collisions [1–3]. In high-energy nuclear collisions, the initial geometric anisotropy is established from the overlap between the colliding nuclei. The time necessary to build up this spatial anisotropy is believed to be short because the colliding nuclei are highly Lorentz contracted in the center-of-mass system and pass through each other at approximately the speed of light. During a $\sim 5\text{--}50$ fm/c period, rescattering transfers the initial spatial anisotropy into a momentum anisotropy. This momentum anisotropy manifests itself most strongly in the azimuthal distribution of transverse momenta. The extent to which the initial spatial anisotropy is transformed to the measured momentum anisotropy depends on the initial conditions and the dynamical evolution of the system. In particular, anisotropy measurements for nucleus-nucleus collisions at RHIC energies may provide information about a partonic stage that may exist early in the collision evolution [1, 4–8].

The transverse momentum distribution of particles can be described in the form:

$$\frac{d^2N}{dp_t^2 d\phi} = \frac{dN}{2\pi dp_t^2} [1 + 2 \sum_n v_n \cos(n\phi)], \quad (1)$$

where p_t is the transverse momentum of the particle, ϕ is its azimuthal angle with respect to the reaction plane [9, 10] and the harmonic coefficients, v_n , are anisotropy parameters. The

second coefficient v_2 is called *elliptic flow*, where flow denotes collective behavior without necessarily implying a hydrodynamic limit. Recent experimental results from RHIC [11–14] include measurements of v_2 as a function of collision centrality and p_t for charged particles with $p_t < 2.0$ GeV/c, and for identified charged pions, kaons and protons for p_t up to ~ 0.8 GeV/c. The degree of the anisotropy transfer from position to momentum distribution depends on the density of the system during its evolution and the scattering cross sections of the particles involved (parton and/or hadron). As a result, recent theoretical work attempted to deduce the initial gluon density from partonic energy loss [6], and the equation of state from hydrodynamic model calculations [5, 7].

Most of the anisotropic flow parameters measured to date are for non-strange particles [11, 12, 15–19]. Of the studies for identified strange particles [12, 20–25] most have been at much lower collision energies. Moreover, previous measurements of strange particle flow correspond to directed flow, *i.e.* the coefficient v_1 . At the CERN SPS, quantitative differences between multi-strange baryons and non-strange hadrons were observed in transverse radial flow in Pb + Pb collisions at $\sqrt{s_{NN}} = 17$ GeV [26, 27]. A physical scenario in which multi-strange baryons do not participate in a common expansion and thus decouple early from the collision system due to their small hadronic cross sections, was proposed to explain this observation [28]. This explanation suggests that it may be possible to obtain insight into very early stages of the col-

lisions by studying the elliptic flow of strange particles.

In this paper, we report the first measurement of the azimuthal anisotropy parameter v_2 for the strange particles K_S^0 , Λ and $\bar{\Lambda}$ from Au + Au collisions at $\sqrt{s_{\text{NN}}} = 130$ GeV. Our measurement of v_2 for different centralities as a function of p_t using the Solenoidal Tracker At RHIC (STAR) extends to a p_t of about 3.0 GeV/c, much higher than previously measured for identified charged pions, kaons and protons [12].

The STAR detector [29], with its azimuthal symmetry and large acceptance, is ideally suited to measure elliptic flow. The detector consists of several sub-systems in a large solenoidal magnet. For collisions in its center, the Time Projection Chamber (TPC) measures charged tracks in the pseudo-rapidity range $|\eta| < 1.5$ with 2π azimuthal coverage. During the year 2000 data taking the STAR magnet operated at a 0.25 Tesla field, allowing tracking of particles with $p_t > 0.075$ GeV/c. A scintillator barrel surrounding the TPC, the Central Trigger Barrel (CTB), measures the charged particle multiplicity (for triggering) from within $|\eta| < 1$. Two zero-degree calorimeters [30] located at ± 18.25 m from the nominal interaction region, sub-tending an angle $\theta < 0.002$ radians, primarily detect fragmentation neutrons. Two ZDCs in coincidence provide a minimum-bias trigger and the CTB is used for a central trigger. This analysis uses 201×10^3 minimum-bias and 180×10^3 central events.

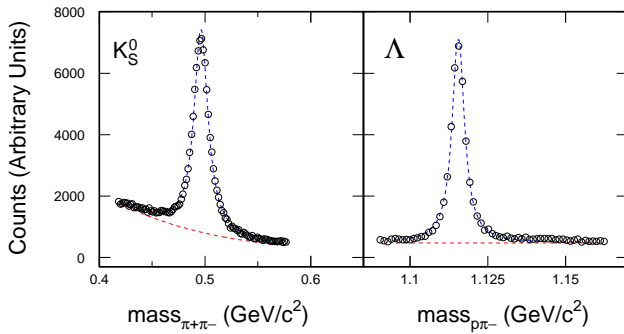


FIG. 1: Invariant mass distributions for $\pi^+\pi^-$ showing a K_S^0 mass peak (left panel) and for $p\pi^-$ showing a Λ mass peak (right panel). Fitting results are shown as dashed lines in the figure. For presentation a greater number of events has been used for the Λ plot.

We reconstructed both $K_S^0 \rightarrow \pi^+ + \pi^-$ and $\Lambda(\bar{\Lambda}) \rightarrow p + \pi^-(\bar{p} + \pi^+)$ from their charged daughter tracks detected in the STAR TPC [31]. Using the energy loss of the charged tracks in the TPC gas, we select candidates for protons, anti-protons and pions. The mass and the kinematic properties of the neutral particle candidates are extracted from the decay vertex and daughter particle kinematics. Fig. 1 shows the invariant mass distributions for $\pi^+\pi^-$ showing a K_S^0 mass peak and for $p\pi^-$ showing a Λ mass peak. The dashed lines are fits to the background and the signal. We determined that the background is dominated by combinatorial counts by rotating all positive tracks 180 degrees in the transverse plane and reconstructing the K_S^0 and $\Lambda(\bar{\Lambda})$ decay vertices. This proce-

dure destroys all real vertices in the TPC acceptance so that we can describe the combinatorial contribution to the invariant mass distributions. The observed masses, 496 ± 8 MeV/c 2 for $\pi^+\pi^-$ and 1116 ± 4 MeV/c 2 for $p\pi$, are consistent with accepted values [32] and the widths are determined by the momentum resolution of the detector. The particles used for the v_2 analysis are from the kinematic region of $|y| \leq 1.0$ and $0.2 \leq p_t \leq 3.2$ GeV/c for K_S^0 or $0.3 \leq p_t \leq 3.2$ GeV/c for $\Lambda + \bar{\Lambda}$, where y is the particle's rapidity. No significant differences in elliptic flow are observed between Λ and $\bar{\Lambda}$, so because of the limited statistics, Λ and $\bar{\Lambda}$ are summed together.

We choose the requirements for K_S^0 and $\Lambda(\bar{\Lambda})$ daughter candidates to maximize statistics. For K_S^0 , we require the daughter tracks to have a distance-of-closest-approach (dca) to the collision vertex > 1.0 cm. For the $\Lambda(\bar{\Lambda})$ reconstruction, we choose pion-like tracks with a dca > 1.5 cm and proton-like tracks with a dca > 0.8 cm. We use the peak in the invariant mass distribution to measure the yield of K_S^0 or $\Lambda + \bar{\Lambda}$ particles for different values of ϕ and p_t . Using the ϕ bin center for the value of ϕ , we evaluate v_2 as a function of p_t by calculating $\langle \cos(2\phi) \rangle$ for different values of p_t . Using the yield to calculate $v_2 = \langle \cos(2\phi) \rangle$ enables us to measure elliptic flow for identified particles beyond the p_t region where the identification of particles via their energy loss in the TPC gas fails [12].

The real reaction plane is not known, but the event plane, an experimental estimator of the true reaction plane, can be calculated from the azimuthal distribution of tracks [11]. To determine the event plane, we select charged particle tracks with at least 15 measured space points, $0.1 < p_t \leq 2.0$ GeV/c and $|\eta| < 1.0$. We also require the ratio of the number of space points to the expected maximum number of space points for each track to be greater than 0.52, suppressing split tracks from being counted twice. Events are required to have a primary vertex within 75 cm longitudinally of the TPC center. These cuts are similar to those used in Ref. [11] and our analysis is not biased by them.

To avoid possible auto-correlations, tracks used for the K_S^0 or $\Lambda(\bar{\Lambda})$ reconstruction are excluded from the set of tracks used to calculate the event plane. Typically this is done by measuring the azimuthal angle between a track and the event plane calculated from all other qualifying tracks within the same event. Then the contribution to v_2 from that track is calculated. In this analysis, where v_2 is not calculated on a particle by particle basis, all tracks that might be used for the reconstruction of K_S^0 or $\Lambda(\bar{\Lambda})$ are excluded from the event plane calculation. Only tracks with a dca < 1.0 cm are used in the event plane calculation while the K_S^0 vertices don't include these tracks. In the $\Lambda + \bar{\Lambda}$ analysis all proton-like tracks are excluded from the event plane calculation. A track is considered proton-like if its energy loss (dE/dx) is within three standard deviations of that expected for protons.

When the azimuthal anisotropy is evaluated via $v_2 = \langle \cos(2\phi) \rangle$, the observed v_2 must be corrected to account for the imperfect event plane resolution [33]. This resolution is influenced by two factors that depend on centrality: the

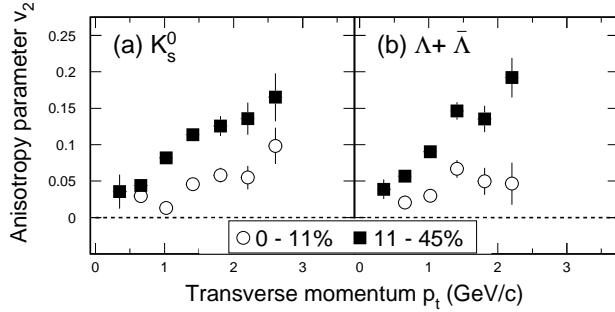


FIG. 2: Elliptic flow v_2 as a function of p_t for (a) K_S^0 and (b) $\Lambda + \bar{\Lambda}$. Circles and filled squares are for central (0–11%) and mid-central (11–45%) collisions, respectively.

strength of the anisotropy signal and the number of tracks used for the event plane calculation. We estimate the resolution using the method of random subevents [10] and use the relative multiplicity, as in Ref. [11], to measure the event centrality. The maximum resolution for the K_S^0 and $\Lambda + \bar{\Lambda}$ analysis is found to be 0.681 ± 0.004 and 0.582 ± 0.007 respectively and is reached in the centrality corresponding to 25–35% of the measured cross section. The relatively lower resolution for the $\Lambda + \bar{\Lambda}$ analysis is caused by the exclusion of proton-like tracks from the event plane calculation.

Elliptic flow as a function of transverse momentum for central and mid-central collisions calculated from 201×10^3 minimum-bias and 180×10^3 central events is shown in Fig. 2. The two particles show a similar p_t dependence in the two centrality intervals. The p_t dependence is stronger in more peripheral collisions than in the central collisions. A similar dependence was observed for charged particles in Au + Au collisions at the same RHIC energy [12].

For this analysis, three main sources contribute to systematic errors in the measured anisotropy parameters: particle identification, background subtraction, and correlations unrelated to the reaction plane (non-flow) such as resonance decays, jets or Coulomb and Bose-Einstein correlations [34, 35]. The contribution from the first two sources is estimated by examining the variation in v_2 after changing several track and event cuts. We estimate that these effects contribute an error of less than ± 0.005 to v_2 . The contribution to v_2 from non-flow effects, however, could be significant, especially in peripheral collisions. A previous study used the correlation of event plane angles from subevents to estimate the magnitude of these contributions [36]. Non-flow effects are assumed to contribute to the first and second harmonic correlations by similar amounts, so the magnitude of the first harmonic correlation sets a limit on the non-flow contributions to v_2 . That study showed that the non-flow systematic errors for charged particles are typically $+0$ and -0.005 , but are significantly larger in the more peripheral events where the error increases to $+0$ and -0.035 for the 58–85% most central events. These estimates are confirmed by measurements of v_2

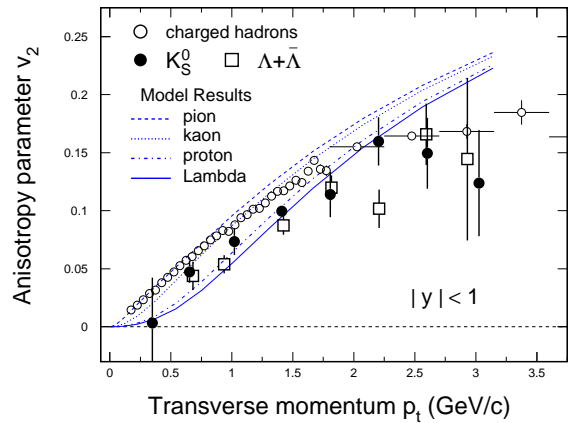


FIG. 3: Elliptic flow v_2 as a function of p_t for the strange particles K_S^0 (filled circle) and $\Lambda + \bar{\Lambda}$ (open squares) from minimum-bias Au+Au collisions. For comparison, v_2 of charged hadrons (open circles) is also shown. The lines are from hydrodynamic model calculations [5].

using the 4th-order cumulant method, a method that is insensitive to non-flow effects but which leads to larger statistical errors [37]. We assume the systematic errors on v_2 for the neutral strange particles K_S^0 and $\Lambda + \bar{\Lambda}$ are similar to those found in the analysis of charged particles [12].

To make a comparison with available hydrodynamic model calculations, we plot $v_2(p_t)$ for both K_S^0 and $\Lambda + \bar{\Lambda}$ from 201×10^3 minimum-bias collisions in Fig. 3. The dashed lines represent the hydrodynamic model calculations [5] for (from top to bottom) pions, kaons, protons, and lambdas. Also shown in the figure is $v_2(p_t)$ for charged hadrons [38]. Within statistical uncertainty, the K_S^0 results are in agreement with the v_2 of charged kaons (not shown) [12]. We observe that v_2 for both strange particles increases as a function of p_t up to about 1.5 GeV/c, similar to the hydrodynamic model prediction. In the higher p_t region however ($p_t \geq 2$ GeV/c), the values of v_2 seem to be saturated. It has been suggested that the shape and height of v_2 above 2 – 3 GeV/c in a pQCD model is related to energy loss in an early, high-parton-density, stage of the evolution [6].

The p_t integrated anisotropy parameters for charged hadrons, K_S^0 , and $\Lambda + \bar{\Lambda}$ from minimum-bias collisions are shown in Fig. 4. The integrated values of v_2 are calculated by parameterizing the yield with the inverse slope parameter of exponential fits to the K_S^0 or $\Lambda + \bar{\Lambda}$ transverse mass distributions [38, 39]. The integrated v_2 is dominated by the region near the particle's mean p_t and is insensitive to the upper and lower bounds of the integration. Although the $v_2(p_t)$ of $\Lambda + \bar{\Lambda}$ is below the $v_2(p_t)$ of K_S^0 for most p_t , as shown in Fig. 3, the p_t integrated v_2 values increase with the particle mass. This increase is partly due to the relatively higher mean p_t of the $\Lambda + \bar{\Lambda}$ compared to the K_S^0 . In hydrodynamic models, although the spatial geometry of the pressure gradient and the resultant collective velocity are the same for all particles, massive particles tend to gain larger transverse momenta and so de-

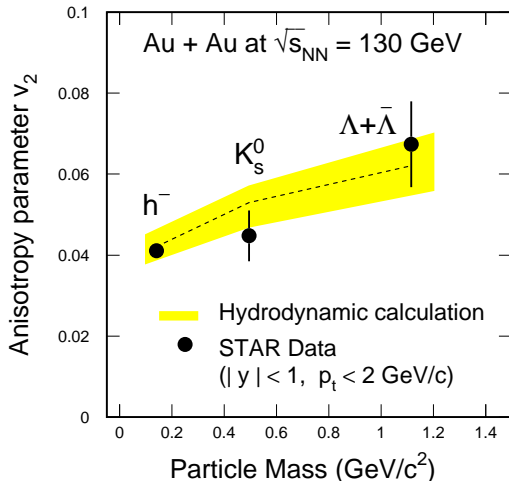


FIG. 4: Integrated elliptic flow v_2 as a function of particle mass. The gray-band and central line indicates the hydrodynamic model results [5].

velop a larger elliptic flow. The hydrodynamic model calculations [5], shown as a gray-band and central line, are, within errors, in agreement with this result. The width of the gray-band in Fig. 4 indicates the uncertainties of the model calculation, mostly due to the choice of the freeze-out conditions. The increase of v_2 with particle mass indicates that significant collective motion, perhaps established early in the collision, is an effective means to transfer geometrical anisotropy to momentum anisotropy. The nature of the particles during this process, however, whether parton or hadron, and the degree of thermalization for strange particles during the collective expansion remains an open issue.

In summary, we have reported the first measurement of the anisotropy parameter, v_2 , for K_S^0 and $\Lambda + \bar{\Lambda}$, from Au + Au collisions at $\sqrt{s_{NN}} = 130$ GeV. The v_2 values as a function of p_t from mid-central collisions are higher at each p_t than v_2 from central collisions. Hydrodynamic model calculations seem to adequately describe elliptic flow of the strange particles up to a p_t of 2 GeV/c. For p_t above 2 GeV/c, however, the observed v_2 seems to saturate whereas hydrodynamic models predict a continued increase with p_t . The p_t integrated v_2 as a function of particle mass is consistent with a hydrodynamic picture where collective motion, established by a pressure gradient, transfers geometrical anisotropy to momentum anisotropy. Although the hadronic scattering cross sections of strange and non-strange particles may be different, we have yet to see deviations in the measured v_2 from hydrodynamic calculations at low p_t for strange or non-strange particles. In a possible partonic phase prior to the hadronic epoch, the hadronic scattering cross sections for the final hadrons are not relevant. As such, if the elliptic flow of identified particles proves to be independent of their relative hadronic cross sections, it may be evidence that v_2 is established during a partonic phase.

Acknowledgments: We thank P. Huovinen for providing the results of the hydrodynamic model calculations. We wish to thank the RHIC Operations Group and the RHIC Computing Facility at Brookhaven National Laboratory, and the National Energy Research Scientific Computing Center at Lawrence Berkeley National Laboratory for their support. This work was supported by the Division of Nuclear Physics and the Division of High Energy Physics of the Office of Science of the U.S. Department of Energy, the United States National Science Foundation, the Bundesministerium fuer Bildung und Forschung of Germany, the Institut National de la Physique Nucleaire et de la Physique des Particules of France, the United Kingdom Engineering and Physical Sciences Research Council, Fundacao de Amparo a Pesquisa do Estado de Sao Paulo, Brazil, the Russian Ministry of Science and Technology and the Ministry of Education of China and the National Natural Science Foundation of China.

-
- [1] H. Sorge, Phys. Rev. Lett. **82**, 2048(1999).
 - [2] H. Sorge, Phys. Lett. **B402**, 251(1997).
 - [3] J.-Y. Ollitrault, Phys. Rev. **D46**, 229(1992).
 - [4] B. Zhang, M. Gyulassy, and C.M. Ko, Phys. Lett. **B455**, 45(1999).
 - [5] P. Huovinen, P.F. Kolb, U. Heinz, P.V. Ruuskanen, and S. Voloshin, Phys. Lett. **B503**, 58(2001).
 - [6] M. Gyulassy, I. Vitev and X.N. Wang, Phys. Rev. Lett. **86**, 2537(2001).
 - [7] D. Teaney, J. Lauret, and E.V. Shuryak, Phys. Rev. Lett. **86**, 4783(2001).
 - [8] Z.W. Lin and C.M. Ko, Phys. Rev. **C65**, 034904(2002).
 - [9] S. Voloshin and Y. Zhang, Z. Phys. **C70**, 665(1996).
 - [10] A.M. Poskanzer and S. Voloshin, Phys. Rev. **C58**, 1671(1998).
 - [11] K.H. Ackermann *et al.*, (STAR Collaboration), Phys. Rev. Lett. **86**, 402(2001).
 - [12] C. Adler *et al.*, (STAR Collaboration), Phys. Rev. Lett., **87**, 182301(2001).
 - [13] R.A. Lacey for the PHENIX Collaboration, Nucl. Phys. **A698**, 559(2002).
 - [14] I. Park *et al.*, (PHOBOS Collaboration), Nucl. Phys. **A698**, 564(2002).
 - [15] W. Reisdorf and H.G. Ritter, Ann. Rev. Nucl. Part. Sci. **47**, 663(1997).
 - [16] N. Herrmann, J. Wessels, and T. Wienold, Ann. Rev. Nucl. Part. Sci. **49**, 581(1999).
 - [17] J. Barrette *et al.* (E877 Collaboration), Phys. Rev. Lett. **73**, 2532(1994).
 - [18] S. Wang *et al.* (EOS Collaboration), Phys. Rev. Lett. **76**, 3911(1996).
 - [19] H. Appelshäuser *et al.*, (NA49 Collaboration), Phys. Rev. Lett. **80**, 4136(1998).
 - [20] J. Ritman *et al.*, (FOPI Collaboration), Z. Phys. **A352**, 355(1995); P. Crochet *et al.*, (FOPI Collaboration), Phys. Lett. **B486**, 6(2000).
 - [21] Y. Shin *et al.*, (KaoS Collaboration), Phys. Rev. Lett. **81**, 1576(1998).
 - [22] M. Justice *et al.*, (EOS Collaboration), Phys. Lett. **B440**, 12(1998).
 - [23] P. Chung *et al.*, (E895 Collaboration), Phys. Rev. Lett. **85**,

- 940(2000); P. Chung *et al.*, (E895 Collaboration), Phys. Rev. Lett. **86**, 2533(2001).
- [24] J. Barrette, *et al.* (E877 Collaboration), Phys. Rev. **C63**, 014902(2001).
- [25] M.M. Aggarwal *et al.*, (WA98 Collaboration) Phys. Lett. **B469**, 30(1999).
- [26] I.G. Bearden *et al.*, (NA44 Collaboration), Phys. Rev. Lett. **78**, 2080(1997).
- [27] E. Andersen *et al.*, (WA97 Collaboration), Phys. Lett. **B433**, 209(1998).
- [28] H. van Hecke, H. Sorge, and N. Xu, Phys. Rev. Lett. **81**, 5764(1998).
- [29] K.H. Ackermann *et al.* (STAR Collaboration) Nucl. Phys. **A661**, 681c(1999).
- [30] C. Adler *et al.*, Nucl. Instrum. Meth. **A461**, 337(2001)
- [31] H. Wieman *et al.* IEEE Trans. Nucl. Sci. **44**, 671 (1997); W. Betts *et al.* IEEE Trans. Nucl. Sci. **44**, 592(1997); S. Klein *et al.*, IEEE Trans. Nucl. Sci. **43**, 1768(1996).
- [32] Particle Data Group (D.E. Groom *et al.*), Eur. Phys. J. **C15**, 1 (2000).
- [33] R. Snellings, A. Poskanzer, and S. Voloshin, STAR Note SN0388(1999); nucl-ex/9904003.
- [34] N. Borghini, P.M. Dinh, and J.Y. Ollitrault, Phys. Lett. **B477**, 51(2000).
- [35] N. Borghini, P.M. Dinh, and J.Y. Ollitrault, Phys. Rev. **C62**, 034902(2000).
- [36] R. Snellings for the STAR Collaboration, Nucl. Phys. **A698**, 193(2002)
- [37] A. H. Tang for the STAR Collaboration, arXiv:hep-ex/0108029
- [38] M. Lamont for the STAR Collaboration, in *Proceedings of Strange Quarks in Matter 2001* (to be published)
- [39] H. Long, Ph.D. Thesis, University of California - Los Angeles, (2002)